MALDI-TOF Characterization of Highly Cross-Linked, Degradable Polymer Networks

Amy K. Burkoth and Kristi S. Anseth*

Department of Chemical Engineering, University of Colorado, Boulder, Colorado 80309-0424

Received September 15, 1998; Revised Manuscript Received December 8, 1998

ABSTRACT: Multifunctional anhydride monomers were synthesized and photopolymerized to form highly cross-linked, degradable networks. The networks were synthesized from monomers and oligomers of dimethacrylated sebacic acid of varying molecular weight, as well as under varying reaction conditions. The cross-linked polymers were subsequently degraded in phosphate buffered saline, and the degradation products, sebacic acid and poly(methacrylic acid), were isolated. Matrix-assisted laser desorption/ionization time-of-flight mass spectrometry (MALDI-TOF MS) was used to characterize the absolute molecular weight distribution of the linear poly(methacrylic acid) degradation product, especially as a function of the network evolution (i.e., double-bond conversion), rate of initiation, and monomer size. MALDI-TOF results, supported by ^{1}H NMR, showed that the distribution of kinetic chain lengths was relatively narrow, with average lengths shorter than calculated from experimentally measured rate data, indicating the influence of diffusion-controlled kinetics as well as chain transfer. Furthermore, the average kinetic chain length shifted to lower values with increasing initiation rate and double-bond conversion. Since multifunctional monomer polymerizations are extremely complex and notoriously difficult to characterize due to the insoluble nature of the resulting cross-linked polymer structure, this work demonstrates, for the first time, how these degradable monomers can provide further insight and characterization of multifunctional monomer polymerizations.

Introduction

Multifunctional monomers that react to form densely cross-linked polymer networks are greatly expanding in their development, use, and application. For example, multifunctional monomers are routinely photopolymerized to produce rapidly highly cross-linked polymers at room temperature without the use of solvents for applications ranging from optical fiber coatings to dental materials. This field alone is a multibillion dollar industry with more than 20% per annum growth, demonstrating the potential and increasingly important role of multifunctional monomers in photopolymerized materials. In general, the resulting cross-linked polymers are increasingly used in applications where mechanical strength and dimensional stability (i.e., resistance to solvent penetration) are essential. For example, the mechanical properties and resistance to swelling of photopolymerized dimethacrylate monomers have led to their application in dentistry.

While the applications for materials formed from multifunctional monomers are continually expanding, the complex reactions that occur during the formation of these highly cross-linked networks are poorly understood. Multifunctional monomers react to form densely cross-linked networks through complex, diffusion-limited polymerization reactions.[1,2] As each monomer reacts and becomes part of the network, the increase in viscosity dramatically affects the mobility of the reacting species. Such diffusion limitations result in unequal reactivity of functional groups,[3−6] limiting double-bond conversions,[7−9] radical trapping,[10−12] and numerous other complex features that convolute the basic understanding of the polymerization kinetics. The insolubility of the evolving cross-linked network structure further limits and complicates experimental investigation of the polymerization. The high cross-linking density makes it difficult to extract unreacted monomer to differentiate between pendant and monomeric double bonds.[9] Furthermore, since the materials are not readily reprocessed after formation, understanding the complex relationship between reaction conditions and the resulting network structure and properties is critically important since the material properties are essentially fixed during formation. Numerous groups[1−4,13−15] are investigating this important problem.

One area of particular interest to our group has been the development and use of multifunctional monomers that can be photopolymerized to form highly cross-linked, *degradable* networks. To this extent, we recently reported a new class of dimethacrylated anhydride monomers which react to form such networks.[16] Our intent was to design monomers that would photopolymerize rapidly in vivo to form stable and surface eroding networks for orthopaedic applications, which would considerably simplify surgical treatments. Previously, we have shown that the aforementioned monomers react to form highly cross-linked networks in seconds to minutes, achieving conversions in excess of 0.95.[16] In addition, we have reported that the rate of surface erosion for these polyanhydride networks is controlled by the chemical composition and can be varied from several days to a year.[17] In general, the mechanical properties of these networks were within the ranges reported for trabecular and cortical bone and maintained greater than 70% of their tensile modulus with 50% mass loss.[17]

While application of these degradable and cross-linked polymers is diverse and exciting, these materials can be further utilized from a fundamental perspective to provide insight into the polymerization behavior of multifunctional monomer systems. Since these dimethacrylated anhydride monomers react to form networks

* To whom correspondence should be addressed.

10.1021/ma9814651 CCC: $18.00 © 1999 American Chemical Society
Published on Web 02/17/1999

with hydrolytically degradable anhydride cross-links, analysis of the degradation products can give insight into the complex network structure and reaction mechanisms. In particular, information about the average number of double bonds consumed (polymerized) per each radical that initiates a polymer chain (kinetic chain length, ν) can be directly measured. The distribution of kinetic chain lengths, especially as a function of conversion, provides insight about the initiation, propagation, and termination mechanisms, as well as the presence of chain transfer. For multifunctional monomer systems, this information was previously unavailable because of the insolubility of the evolving network structure. Hence, these new monomers that form degradable networks upon reaction provide a unique opportunity to obtain experimental information regarding the mechanisms of chain growth by analysis of the linear degradation products. Characterization of the degradation products is also of practical importance in medical applications of these networks since there is a maximum accumulation in the circulatory system for polymers over a critical molecular weight of 200 000, regardless of polymer type.[18]

Hence, this work presents matrix-assisted laser desorption/ionization time-of-flight mass spectrometry (MALDI-TOF MS) analysis of the molecular weight distribution of poly(methacrylic acid) degradation products of highly cross-linked networks produced from dimethacrylated sebacic acid. MALDI-TOF MS is a new analytical technique which has, until recent, been used as a tool for characterizing high molecular weight biomolecules, such as proteins and oligonucleotides.[19,20] More recently, it has become popular as a molecular weight tool for synthetic polymers, providing absolute measures of the molecular masses rather than relative ones.[21−23] MALDI-TOF can provide molecular weight distributions of linear polymers more quickly and accurately than conventional techniques. Thus, this work verified that MALDI-TOF could be used to characterize the distribution of kinetic chain lengths in these degradable systems. Then, the effects of degree of double-bond conversion, rate of initiation, and monomer size on the molecular weight distribution of degradation products were investigated to provide insight regarding the complexities of multifunctional monomer polymerizations.

Experimental Section

Methacrylated sebacic anhydride (MSA) was synthesized by refluxing sebacic acid (Aldrich) in 2.5 equiv of methacrylic anhydride (Aldrich) at 80 °C for approximately 1 h. The MSA product was subsequently purified by removing excess methacrylic anhydride and the methacrylic acid byproduct by rotavapping and precipitating in petroleum ether from a methylene chloride solution. Methacrylate $=CH_2$ protons were confirmed with ^{1}H NMR at approximately $\delta = 6.0$ and 6.5 ppm. Comparing the $=CH_2$ protons to the internal methylene protons of the sebacic acid, we calculated approximately 3 sebacic acid repeat units (m) between the methacrylate end groups (MW $\cong$ 707 g/mol). To form higher molecular weight monomers, the MSA was oligomerized by melt condensation at 100 °C for 90 min under vacuum. The degree of oligomerization, as quantified by ^{1}H NMR, was approximately 13 sebacic acid repeat units between the methacrylate end groups.

Samples were polymerized with an ultraviolet light source (EFOS, Ultracure 100SS) at light intensities of either 10 or 100 mW/cm^2. A band-pass filter was used in conjunction with the light source to provide a majority of the light at 365 nm. All light intensities were measured with a radiometer (Spot-Cure intensity meter, Instrumentation Products). All photopolymerizations were initiated with 0.1 wt % 2,2-dimethoxy-2-phenylacetophenone (DMPA, Ciba Geigy), a common photoinitiator used in many ultraviolet photopolymerizations.[1] From a practical standpoint, using a small amount of initiator is important for reducing light attenuation in the sample. For samples initiated with 0.1 wt % DMPA, 94% of the light is transmitted to a depth of 1 mm as compared to only 56% in samples initiated with a 1.0 wt % initiator. DMPA was dissolved in the chosen monomer/oligomer at an elevated temperature (~70 °C), and the resulting solution was transferred into a Teflon mold and subsequently photopolymerized to produce disks approximately 1 mm in thickness and 14 mm in diameter. The polymerization time was estimated by previous IR and ATR experiments.[16]

One-dimensional degradation rates of the polymer disks were characterized by mass loss in phosphate buffered saline at pH 7.4 and 37 °C with orbital shaking at 80 rpm. Degradation products were protonated with concentrated hydrochloric acid and subsequently dried. The solid sebacic acid and poly(methacrylic acid) (PMAA) degradation products were then dissolved in a dimethylformamide (DMF) solution to separate them from the buffer salts. Although sebacic acid has a slight solubility in water (1 mg/mL),[24] water was used to separate the bulk of the sebacic acid degradation products from the desired PMAA.

A differential scanning photocalorimeter (DPC, Perkin-Elmer DSC7) was used to follow the polymerization behavior under a variety of photoinitiation conditions. Neutral density filters (Melles Griot) were used to control the light intensity and obtain photoinitiation conditions similar to those in the degradation studies (0.1 wt % DMPA and 10 or 100 mW/cm^2 ultraviolet light). DSC experiments were run isothermally at 37 °C in the presence of oxygen, simulating in vivo polymerization conditions. The rate of polymerization (R_p) was calculated using the theoretical heat of reaction for methacrylate groups. From the rate data, the kinetic chain length, ν, can be calculated to give a measure of the polymer size as a function of exposure time and is defined as the average number of double bonds consumed by each radical that initiates a polymer chain before it terminates.[25] Neglecting chain transfer and assuming a steady-state radical concentration and uniform illumination (i.e., photopolymerization of a thin film), the kinetic chain length is given by[25]

$$\nu = \frac{R_p}{2\phi\epsilon I_0 b[\mathrm{In}]} \tag{1}$$

where ϕ is the quantum yield for initiation, ϵ is the molar absorptivity, I_0 is the incident light intensity (in moles of light quanta per volume−time), b is the thickness of the system being irradiated, and [In] is the initiator concentration. We have used the following values for DMPA in our calculations: $\phi = 0.6$ and $\epsilon = 150$ L/(mol cm). The kinetic chain length was evaluated as a function of time using the polymerization rate, as measured by DSC, and the calculated initiation rate. It is important to note that the aforementioned equation does not account for polymer chain growth after the UV exposure has been shuttered (i.e., dark polymerization). Decker[26] has investigated the implications of the dark reaction elsewhere.

Matrix-assisted laser desorption/ionization time-of-flight mass spectrometry (MALDI-TOF MS, PerSeptive Biosystems Voyager-DE STR) was used to characterize the molecular weight distribution of PMAA degradation products. The MALDI-TOF instrument was equipped with a nitrogen laser emitting at 337 nm with a 3 ns pulse width. Irradiance intensity and accelerating voltage (10−20 kV) were optimized for each sample. In all cases, negative ions were detected and sinapinic acid (Hewlett-Packard) was used as matrix material. MALDI-TOF samples were prepared by dissolving the PMAA in methanol or water (~10 mg/mL) and mixing in a 1:3 ratio (sample:matrix) by volume. One microliter of this solution was spotted on the sample plate and allowed to evaporate before any additional spots were added. Approximately, a total

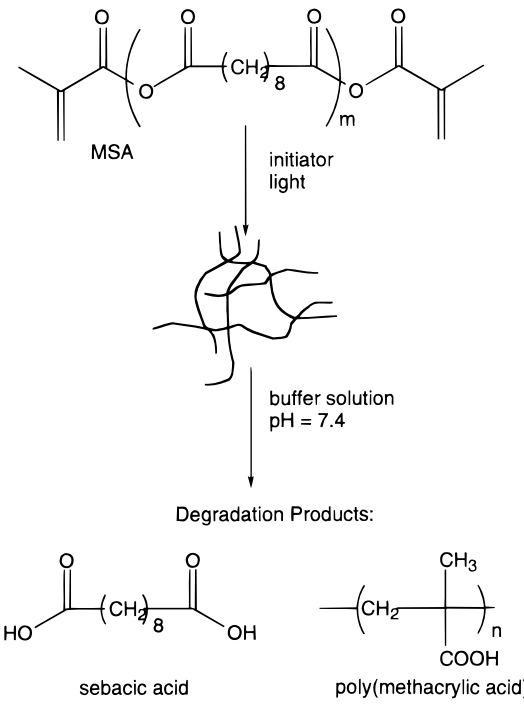

Figure 1. General polymerization and degradation scheme for anhydride monomers and oligomers.

volume of 3 μL was spotted per sample well. The number fraction of *n*-mers was calculated using peak heights.

Proton NMR spectroscopy (Varian VSR-300S) was used to characterize the number-average degree of polymerization ($\overline{n_n}$) of the poly(methacrylic acid) degradation products from the aromatic protons of one of the initiator fragments with NMR at $\delta = 7.5-8.0$ and $\delta = 8.0-8.5$ ppm. The integral values for these peaks ratioed by the methyl protons in the methacrylic acid repeat unit at $\delta = 2.3$ ppm allowed for the calculation of $\overline{n_n}$ to verify the MALDI-TOF results.

Results and Discussion

The dimethacrylated anhydride monomers presented herein photopolymerize to form highly cross-linked and degradable networks. The combination of these monomers' hydrophobic backbone and hydrolytically labile anhydride linkages results in a surface eroding degradation mechanism. The rate of hydrolytic degradation can be varied by altering the degree of hydrophobicity in the backbone substituents. For this study, we have focused on a relatively hydrophilic monomer, MSA, to facilitate timely experimental data collection. However, methacrylated 1,6-bis(carboxyphenoxy)hexane (MCPH) is a more hydrophobic anhydride monomer which degrades significantly slower. From an application standpoint, copolymers consisting of MSA and MCPH can be used to tailor the degradation rate depending on the final network.[17] Furthermore, the high concentration of double bonds in these systems results in a tightly cross-linked structure which aids in the surface degradation mechanism by minimizing solvent transport and swelling of the matrix. In addition to this dimensional stability, the cross-links also increase the mechanical strength of the network, making these materials promising for orthopaedic, load-bearing applications.

The general scheme for the polymer synthesis and degradation is shown in Figure 1. Monomers (or oligomers) were combined with a photoinitiator and, upon irradiance, photopolymerized into a cross-linked network. The anhydride linkages degrade readily upon contact with water, and the entire network degrades from the surface inward, producing sebacic acid and poly(methacrylic acid). The general synthesis described in Figure 1 is applicable to numerous multiacid compounds.[27,28] The backbone chemistry may be modified easily to produce monomers of varying stiffness, size, and functionality (e.g., trimethacrylates and imide-containing dimethacrylates). Characterization of the molecular weight distribution of the PMAA degradation products, especially as a function of the polymerizing conditions, was a primary focus of this work. However, the adaptability of this synthesis should allow for the characterization of many effects of monomer structure on network evolution during multifunctional monomer polymerizations.

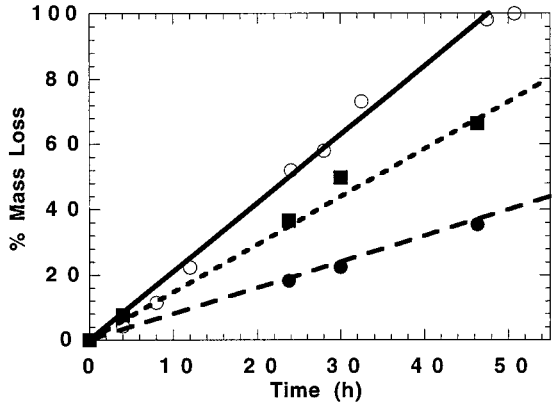

Figure 2. Degradation behavior of MSA ($m \sim 3$) (○) and oligomerized MSA, $m \sim 7$ (■) and $m \sim 11$ (●).

Figure 2 illustrates a typical degradation profile as seen in these cross-linked polyanhydride disks. The disks approximate one-dimensional degradation, so the linear mass loss profile confirms the surface erosion mechanism, and the rate of degradation depends strongly on the network composition. Methacrylated sebacic acid ($m \sim 3$) networks degrade in approximately 50 h. This rate is considerably slower than linear poly(sebacic acid), which degrades in approximately 25 h.[29] While cross-linking clearly slows the degradation rate by increasing the resistance to water penetration, poly(methacrylic acid) degradation products from the cross-linked networks are relatively hydrophilic and can potentially accelerate the degradation depending on its concentration relative to the more hydrophobic degradation product, sebacic acid. That is, the final degradation rate is influenced by both the cross-linking density and the composition of the network. To this extent, we investigated these effects by oligomerizing our monomers, which decreases both the cross-linking density of the final network and the amount of poly(methacrylic acid) formed during degradation. The results shown in Figure 2 demonstrate that the overall degradation rate is significantly slowed by reducing the hydrophilic degradation products despite the lower cross-linking density. While the poly(MSA) disk is completely degraded in 48 h, the disks synthesized from oligo(MSA) with 7 and 11 sebacic acid repeat units are degraded much more slowly, taking 69 and 125 h, respectively. Furthermore, the tensile modulus of the final networks, as measured by dynamic mechanical analysis, was not significantly diminished despite the decrease in cross-linking density with oligomerization. In general, all of the oligomers studied formed highly cross-linked, glassy

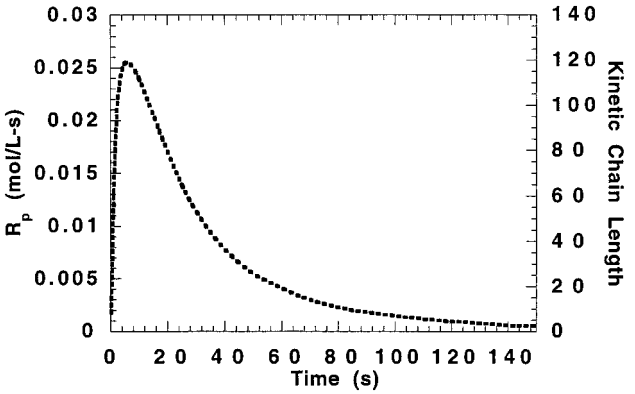

Figure 3. Rate of polymerization and instantaneous kinetic chain length as a function of time for MSA photopolymerized with 100 mW/cm^2 of ultraviolet light.

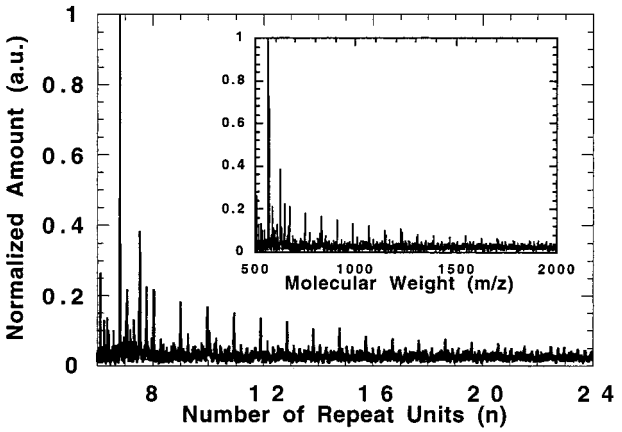

Figure 4. MALDI-TOF MS distribution of PMAA degradation products as a function of degree of polymerization for MSA photopolymerized with 100 mW/cm^2 of ultraviolet light to ~80% conversion.

polymer networks at 37 °C with tensile moduli between 300 and 700 MPa.

While multifunctional monomers that react to form high-strength, degradable, and cross-linked networks can provide many benefits, especially in biomedical applications, these materials are also highly useful in characterizing the fundamentals of multifunctional monomer polymerizations. Because the resulting networks are degradable, analysis of the degradation products can provide new insight regarding the complex network structure and the diffusion-controlled reactions that dominate the network evolution. In general, these dimethacrylated anhydride monomers have similar polymerization reaction behavior compared to other multifunctional monomers,[30,31] and a typical rate curve is shown in Figure 3 for the photopolymerization of MSA. In general, the polymerization reaction is complicated by diffusion-controlled kinetics, with a nearly immediate onset of autoacceleration. As conversion and viscosity continue to increase, autodeceleration results whereby propagation becomes diffusion limited and the rate of polymerization decreases. Eventually, a limiting conversion is reached, where radicals and unreacted double bonds become trapped in the network and the polymerization rate becomes vanishingly small. Despite continued initiation, the low mobility in the highly cross-linked network prevents further conversion. From a practical standpoint, the photopolymerizations are nearly complete, with the bulk of the double bonds reacted, in 60 s. The final conversion, as measured with IR spectroscopy[16] under these reaction conditions, was 0.80. In addition, the instantaneous kinetic chain lengths are shown, demonstrating that a range of kinetic chain lengths up to 120 units can be expected from these polymerizing conditions. While chain transfer is well-known to decrease molecular weights, diffusion limitations can affect the molecular weight distribution in a complex manner by influencing both the propagation and termination kinetic constant.

Upon completion of the polymerization, the resulting cross-linked networks were degraded, and the molecular weight distribution of the poly(methacrylic acid) degradation products were analyzed to provide insight into the polymerization kinetics. PMAA is a water-soluble, linear polymer which can be analyzed by many methods; however, this work has focused on using MALDI-TOF MS as a tool for the determination of PMAA molecular mass distributions. A typical MALDI-TOF spectrum is shown in Figure 4. This spectrum is for the PMAA degradation products of a poly(MSA) sample which was polymerized at 100 mW/cm^2 until the reaction was essentially complete ($X = 0.80$). The monomeric repeat unit is clearly resolved, and the spectrum visibly extends from chains with $n = 5$ to $n = 24$. Clearly, the kinetic chain lengths as measured by MALDI-TOF are much shorter than those predicted by the simple DSC calculation. This difference is attributed partially to the diffusion limitations in these multifunctional monomer polymerizations as well as to the presence of chain transfer, which may further narrow the distribution and shift it to lower molecular weights.

Also of interest are the smaller peaks that appear between the peaks associated with the monomeric repeat units. These small peaks may be due to different initiator fragments that have added to the PMAA chain to initiate polymerization. The initiator used, DMPA, undergoes a Norrish type 1 cleavage whereby two asymmetric radicals are formed.[32] In addition, termination may occur by disproportionation or combination leading to either one or two of the initiator fragments per chain, respectively. These effects result in multiple combinations of initiator end groups which are visible in the MALDI-TOF spectra. Furthermore, one series of peaks may be a loss of water as seen commonly with poly(acrylic acid).[33] Chain transfer to the methyl protons on the PMAA backbone may also occur and would further produce peaks that vary from the monomeric repeat unit.

While MALDI-TOF is often an exceptional tool for analyzing the end groups and side chains of synthetic polymers, the analysis of such fragments for our PMAA chains is beyond the scope of this paper. Instead, this work aims to look at several factors that may influence the molecular weight distribution of kinetic chain lengths in highly cross-linked networks. First, the influence of double-bond conversion on the distribution of the PMAA chains was investigated by photopolymerizing MSA networks under identical initiating conditions, but to different conversions. The first system was reacted until a maximum double-bond conversion was reached ($X_{max} \sim 0.80$) by exposing to 100 mW/cm^2 of ultraviolet light for 5 min. The second was only partially reacted ($X \sim 0.40$) by exposing for 15 s and then removing the light source.

Figure 5 compares the data from two MALDI-TOF spectra for the degradation of these poly(MSA) samples at low and high double-bond conversion. In Figure 5,

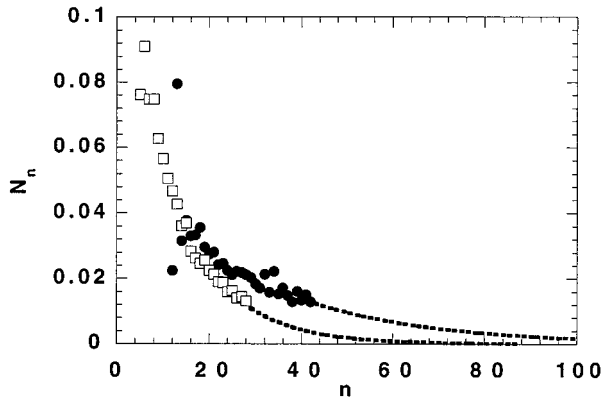

Figure 5. MALDI-TOF distribution of the number fraction of *n*-mers, N_n, as a function of *n* for two samples of varied conversion: MSA polymerized to 40% (●) and 80% (□) double-bond conversion with 100 mW/cm^2 of ultraviolet light.

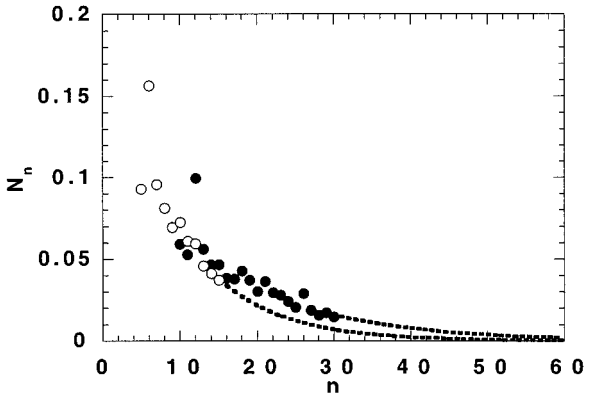

Figure 6. MALDI-TOF distribution of the number fraction of *n*-mers, N_n, as a function of *n* for two samples polymerized with differing initiation rates: oligo(MSA) photopolymerized with 10 (●) and 100 mW/cm^2 (○) of ultraviolet light.

the number fraction of *n*-mers N_n is plotted as a function of the number of monomeric repeat units per chain (*n*). Due to the noise in the spectra at high molecular weights, the tails of the degradation product curves were fit exponentially to extrapolate the number fraction of high molecular weight chains. The dashed lines represent the fitted data. In these experiments, the collected data are a cumulative distribution of all the kinetic chains formed to that point in the polymerization.

Several features are important to note in the distributions of the kinetic chain lengths with conversion. The MSA network which was allowed to polymerize to high conversion had a distribution that was shifted to significantly lower molecular weights compared to the poly(MSA) that was only partially reacted. The number-average kinetic chain length ($\overline{n_n}$) as measured by MALDI-TOF was 17 and 37 for the networks reacted to high ($X_{max} \sim 0.80$) and low ($X \sim 0.40$) conversion, respectively. This result can be explained, in part, by the diffusion limitations in the reacting system. At low conversions where autoacceleration is predominant, mobility of small molecules is still relatively high and double bonds can diffuse readily to local radicals, and longer chains are formed. At higher conversions, however, propagation becomes diffusion limited, and this limited mobility leads to shorter kinetic chains as radicals are likely to become trapped or terminated after only a few propagation steps.

In addition to the influence of conversion on the number-average degree of polymerization, $\overline{n_n}$, the distributions seen in Figure 5 are relatively narrow, most likely due to the limited mobility in these highly cross-linked systems. The sample reacted to 40% conversion had a more narrow distribution ($Q = 1.28$) than the sample that was polymerized to 80% conversion ($Q = 1.50$). The increase in polydispersity accompanied by a decrease in the average kinetic chain length as the conversion is increased results from the diffusion limitations on the propagating chains. Chains initiated at higher conversions will, on average, be much shorter than chains borne at low conversion. This leads to both a broadening and shift in the distribution to lower kinetic chain lengths. A systematic study of the kinetic chain length distribution coupled with kinetic data should provide a great deal of insight into the complex reactions of multifunctional monomers.

In addition to the effects of conversion on the kinetic chain length distribution, the effects of the rate at which the polymerization was initiated were also examined. The rate of initiation controls the rate at which radicals are generated in the system and, therefore, affects the rate of radical termination. As such, changes in the initiation rate may dramatically influence the distribution of kinetic chain lengths. To quantify these effects, oligo(MSA) was polymerized at two differing initiation rates to approximately 70% conversion. Specifically, one sample was initiated with 100 mW/cm^2 of UV light while the other sample was initiated with 10 mW/cm^2, representing a 10-fold change in the rate of initiation. Both samples had the same double-bond concentration (i.e., monomer size) and the same concentration of photoinitiator (0.1 wt % DMPA). Figure 6 shows the effect that the rate of initiation had on the distribution of kinetic chain lengths during the polymerization of oligo(MSA) as measured by MALDI-TOF. The results show that the distribution is shifted to lower molecular weight chains for the system cured at the high light intensity compared to the sample polymerized at the low light intensity. The calculated number-average kinetic chain lengths were 23 and 14 for the samples initiated at 10 and 100 mW/cm^2, respectively. While the higher light intensity initiates more radicals to propagate, the high concentration of radicals increases the rate of termination, and the end result is a distribution of chains with a lower degree of polymerization. However, the polydispersities of these samples were not dramatically different ($Q = 1.4 \pm 0.05$). Furthermore, combining the kinetic chain length characterization with mechanical property data may provide further insight into the relationship between structure and resulting polymer mechanics.

Finally, the effect of monomer size on the distribution of the degradation products was also investigated. Monomer size, or the distance between functional groups, can have a significant effect on the mobility and reactivity of pendant and monomeric double bonds and, thus, influence the kinetic chain length of the propagating radicals. In addition, an increase in the monomer size decreases the concentration of methacrylate functionalities and may lead to a monomer system that becomes diffusion-limited later in the polymerization (at higher conversions) than a system with a higher concentration of methacrylate double bonds. The MALDI-TOF spectra of degradation products for MSA ($m \sim 3$) and oligo(MSA) ($m \sim 13$) cured at 100 mW/cm^2 are compared in Figure 7. The distributions of PMAA chains were not dramatically different between the two mono-

Table 1. Comparison of the Number-Average Degree of Polymerization for the PMAA Chains As Measured by MALDI-TOF and ^{1}H NMR

monomer	light int (mW/cm^2)	conversion	MALDI $\overline{n_n}$	^{1}H NMR $\overline{n_n}$	MALDI polydispersity (Q)
MSA	100	0.40	37	NA	1.28
MSA	100	0.80	17	13−27	1.50
oligo(MSA)	100	0.70	14	11−21	1.46
oligo(MSA)	10	0.70	23	27−53	1.35

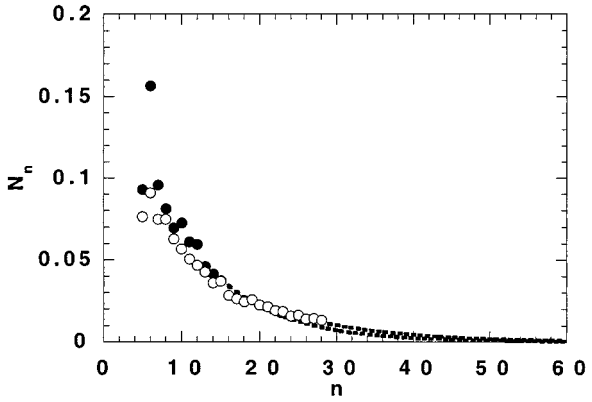

Figure 7. MALDI-TOF distribution of the number fraction of n-mers, N_n, as a function of n for two samples with varied monomer size: for MSA (○) and oligo(MSA) (●) cured with 100 mW/cm^2 of ultraviolet light.

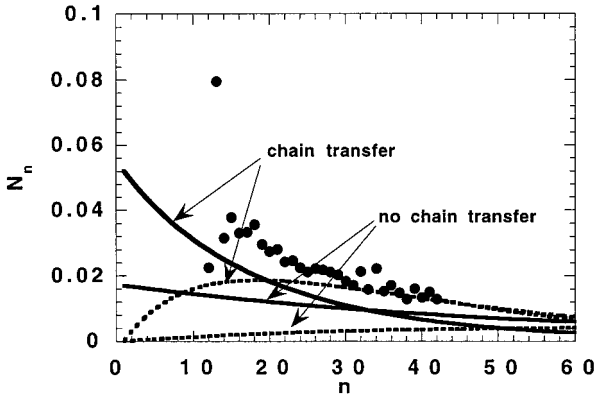

Figure 8. Comparison of MALDI-TOF data (●) for an MSA sample cured with 100 mW/cm^2 of ultraviolet light to ∼40% conversion to the Flory most probable distribution: Dashed lines indicate termination by combination, and solid lines indicate termination by disproportionation. The rate of chain transfer was set equal to 0.001 mol/(L s).

mers of the lengths studied; $\overline{n_n}$ values calculated from the MALDI-TOF data were 17 and 14 for MSA and oligo(MSA) samples, respectively. Furthermore, the polydispersity of the two distributions were approximately the same at 1.5. While the difference in $\overline{n_n}$ between MSA and oligo(MSA) kinetic chain lengths is relatively small, such effects may be more pronounced and important in monomers with a stiffer backbone (e.g., methacrylated 1,6-bis(carboxyphenoxy)hexane) or higher molecular weight.

While the radical polymerizations that form these highly cross-linked networks are extremely complex, it is useful to illustrate the nonidealities of these systems by comparing the experimental results to an ideal distribution such as Flory's most probable distribution. The equations for Flory's distribution are derived by evaluating the probability that a chain will contain n structural units. The number fraction of n-mers with termination by disproportionation (2) or combination (3) is given by[25]

$$N_n = (1 - p)p^{n-1} \tag{2}$$

$$N_n = (1 - p)^2(n - 1)p^{n-2} \tag{3}$$

where N_n is the number fraction of n-mers, n is the number of repeat units, and p is the probability that the radical will propagate rather than terminate (defined as the rate of polymerization divided by the sum of the rates of polymerization, termination, and chain transfer). To compare our MALDI-TOF data to this idealized distribution, we first assumed a pseudo-steady-state approximation for the radical species, and thus, the rate of termination was set equal to the rate of initiation. Then, we used the DSC data along with calculated values for R_i that corresponded to the experimental conditions to calculate p as a function of time. Chain transfer was initially neglected. Since the MALDI-TOF data are an integral distribution for all chains formed throughout the polymerization, the instantaneous most probable distributions were weighted to account for the number of new chains initiated in each time interval and summed to calculate the cumulative distribution.

A comparison of the distribution of kinetic chain lengths as measured by MALDI-TOF with the most probable distribution is shown in Figure 8 for a poly(MSA) sample that was polymerized at 100 mW/cm^2 until approximately 40% functional group conversion. In general, as one might expect, the MALDI-TOF data for these nonideal multifunctional monomer polymerizations deviate significantly from the ideal case. The average number of methacrylic acid repeat units per chain measured experimentally was 37, compared to 55 and 91 for the most probable distribution where termination occurs by disproportionation or combination, respectively. If the influence of chain transfer is considered, a rate of chain transfer (R_{tr} = 0.001 mol/(L s)), which is ∼0.1R_p, significantly shifts the distribution to lower molecular weights. At this rate of chain transfer, $\overline{n_n}$ shifts to 20 for termination by disproportionation and 40 for combination, illustrating that this mechanism may be occurring to a large extent in these dimethacrylated anhydride monomers.

To verify the MALDI-TOF results, ^{1}H NMR was used. Since DMPA fragments into two asymmetric initiator fragments, one with phenyl protons which are shifted significantly downfield (near 8 ppm) from any PMAA protons, ^{1}H NMR was used to calculate the average molecular weight range for the PMAA chains based on probabilities for termination by combination and disproportionation, where the latter mode results in chains with an average molecular weight that is half of the former. Table 1 compares the values of $\overline{n_n}$ as measured by MALDI-TOF to those measured by ^{1}H NMR. With one exception, the $\overline{n_n}$ values calculated from MALDI-TOF fall within the range determined by NMR, further

validating the use of MALDI-TOF MS to characterize these systems.

Conclusions

Dimethacrylated anhydride monomers were investigated that react through complex, diffusion-controlled reactions to form highly cross-linked polymers. While these monomers photo-cross-link to form high strength and biodegradable networks, which make them ideal for drug delivery or orthopaedic applications, degradation products of these networks can be analyzed by MALDI-TOF MS to give insight into the complexities of multifunctional monomer polymerizations. This work demonstrates that MALDI-TOF MS can be used to characterize the absolute distribution of kinetic chain lengths in highly cross-linked polyanhydride networks by examining the distribution of PMAA degradation products. Preliminary MALDI-TOF experiments show that the PMAA distributions span a mass range from 500 to 3500 Da and are influenced significantly by the extent of polymerization (double-bond conversion) and the rate at which the chains are initiated. The number-average degree of polymerization, as calculated by MALDI-TOF MS and confirmed by NMR, for such distributions were shown to decrease with increased double-bond conversion and rate of initiation. Due to the flexible nature of the monomers studied in this work, there was little influence of monomer length on the distribution of the PMAA chains. In a comparison to the Flory most probable distribution, these polymerizations deviate significantly, illustrating the nonidealities associated with the diffusion-controlled kinetics in these multifunctional monomer polymerizations.

Acknowledgment. This work was supported through grants from the National Science Foundation (BES-9734236) and the National Institutes of Health (R29 AR44375).

References and Notes

(1) Kloosterboer, J. G. *Adv. Polym. Sci.* **1984**, *84*, 1−61.
(2) Decker, C. *Polym. Int.* **1998**, *45*, 133−141.
(3) Dusek, K., MacKnight, W., Dickie, R. A., Labana, S. S., Bauer, R. S., Eds. *ACS Symp. Ser.* **1988**, *No. 367*.
(4) Anseth, K. S.; Wang, C. M.; Bowman, C. N. *Polymer* **1994**, *35*, 3243.
(5) Landin, D. T.; Macosko, C. W. *Macromolecules* **1988**, *21*, 846.
(6) Selli, E.; Bellobono, I. R. *Polymerisation Mechanisms*; Elsevier Applied Science: London,, 1993; Vol. 3.
(7) Moore, J. E. In *Chemistry and Properties of Crosslinked Polymers*; Academic Press: New York, 1977.
(8) Simon, G.; Allen, P.; Bennett, D.; Williams, D.; Williams, E. *Macromolecules* **1989**, *22*, 3555.
(9) Kloosterboer, J.; Lijten, G.; Boots, H. *Makromol. Chem., Macromol. Symp.* **1989**, *24*, 223.
(10) Garrett, R. W.; Hill, D. J. T.; O'Donnell, J. H.; Pomery, P. J.; Winzor, C. L. *Polym. Bull.* **1989**, *22*, 611.
(11) Zhu, S.; Tian, Y.; Hamielec, A. E.; Eaton, D. R. *Macromolecules* **1990**, *23*, 1144.
(12) Li, D.; Zhu, S.; Hamielec, A. E. *Polymer* **1993**, *34*, 1383.
(13) Zhu, S.; Hamielec, A. E. *Macromolecules* **1993**, *26*, 3131−3136.
(14) Matsumoto, A. *Adv. Polym. Sci.* **1995**, *123*, 41−80.
(15) Nelson, E. W.; Scranton, A. B. *J. Polym. Sci., Polym. Chem.* **1996**, *34*, 403.
(16) Svaldi-Muggli, D.; Burkoth, A. K.; Keyser, S. A.; Lee, H. R.; Anseth, K. S. *Macromolecules* **1998**, *31*, 4120−4125.
(17) Svaldi Muggli, D.; Burkoth, A. K.; Anseth, K. S. *J. Biomed. Mater. Res.*, in press.
(18) Murakami, Y.; Tabata, Y.; Ikada, Y. *Drug Delivery* **1996**, *3*, 231−238.
(19) Hillenkamp, F.; Karas, M.; Beavis, R. C.; Chait, B. T. *Anal. Chem.* **1991**, *63*, 1193−1202.
(20) Cotter, R. J. *Anal. Chem.* **1992**, *64*, 1027−1039.
(21) Belu, A. M.; DeSimone, J. M.; Linton, R. W.; Lange, G. W.; Friedman, R. M. *J. Am. Soc. Mass Spectrom.* **1996**, *7*, 11−24.
(22) Weidner, S.; Kuhn, G.; Just, U. *Rapid Commun. Mass Spectrom.* **1995**, *9*, 697−702.
(23) Schriemer, D. C.; Liang, L. *Anal. Chem.* **1996**, *68*, 2721−2725.
(24) Domb, A. J.; Nudelman, R. *Biomaterials* **1995**, *16*, 319−323.
(25) Odian, G. *Principles of Polymerization*, 3rd ed.; John Wiley & Sons: New York, 1991.
(26) Decker, C. *Macromolecules* **1990**, *23*, 5217−5220.
(27) Young, J. Ph.D. Dissertation, Chemical Engineering Department, University of Colorado, 1998.
(28) Svaldi-Muggli, D. M. S. Dissertation, University of Colorado, 1997.
(29) Domb, A. *Adv. Polym. Sci.* **1993**, *107*, 93.
(30) Cook, W. D. *J. Polym. Sci., Part A: Polym. Chem.* **1993**, *31*, 1053−1067.
(31) Anseth, K. S.; Kline, L. M.; Walker, T. A.; Anderson, K. J.; Bowman, C. N. *Macromolecules* **1995**, *28*, 2491.
(32) Kurdikar, D.; Peppas, N. A. *Polymer* **1994**, *35*, 1004.
(33) Danis, P. O.; Karr, D. E.; Mayer, F.; Holle, A.; Watson, C. H. *Org. Mass Spectrom.* **1992**, *27*, 843−846.

MA9814651